Bidirectional tumor/stroma crosstalk promotes metastasis in mesenchymal colorectal cancer

Ouahoud, S.; Voorneveld, P.W.; Burg, L.R.A. van der; Jonge-Muller, E.S.M. de; Schoonderwoerd, M.J.A.; Paauwe, M.; ... ; Hardwick, J.C.H.

Oncogene
https://doi.org/10.1038/s41388-020-1157-z

ARTICLE

Bidirectional tumor/stroma crosstalk promotes metastasis in mesenchymal colorectal cancer

Sarah Ouahoud[1] · Philip W. Voorneveld[1] · Lennart R. A. van der Burg[1] · Eveline S. M. de Jonge-Muller[1] · Mark J. A. Schoonderwoerd[1] · Madelon Paauwe[1] · Thijs de Vos[1] · Sophie de Wit[1] · Gabi W. van Pelt[2] · Wilma E. Mesker[2] · Lukas J.A.C. Hawinkels[1] · James C. H. Hardwick[1]

Received: 28 May 2019 / Revised: 13 December 2019 / Accepted: 10 January 2020

Abstract

Patients with the mesenchymal subtype colorectal cancer (CRC) have a poor prognosis, in particular patients with stroma-rich tumors and aberrant SMAD4 expression. We hypothesized that interactions between SMAD4-deficient CRC cells and cancer-associated fibroblasts provide a biological explanation. In transwell invasion assays, fibroblasts increased the invasive capacity of SMAD4-deficient HT29 CRC cells, but not isogenic SMAD4-proficient HT29 cells. A TGF-β/BMP-specific array showed BMP2 upregulation by fibroblasts upon stimulation with conditioned medium from SMAD4-deficient CRC cells, while also stimulating their invasion. In a mouse model for experimental liver metastasis, the co-injection of fibroblasts increased metastasis formation of SMAD4-deficient CRC cells ($p = 0.02$) but not that of SMAD4-proficient CRC cells. Significantly less metastases were seen in mice co-injected with BMP2 knocked-down fibroblasts. Fibroblast BMP2 expression seemed to be regulated by TRAIL, a factor overexpressed in SMAD4-deficient CRC cells. In a cohort of 146 stage III CRC patients, we showed that patients with a combination of high stromal BMP2 expression and the loss of tumor SMAD4 expression had a significantly poorer overall survival (HR 2.88, $p = 0.04$). Our results suggest the existence of a reciprocal loop in which TRAIL from SMAD4-deficient CRC cells induces BMP2 in fibroblasts, which enhances CRC invasiveness and metastasis.

Introduction

For decades, the focus of cancer research has been almost exclusively on epithelial tumor cells. In the past few years, however, there has been a major shift toward the study of the influence of the tumor microenvironment on tumor progression. Crucial new evidence pointing toward a critical role for the tumor microenvironment comes from a series of high-profile gene expression analysis. These studies aimed at classifying colorectal cancer (CRC) according to their gene expression profiles and linking this to prognosis and response to therapy [1]. The poor prognosis of the stroma-rich "mesenchymal CRC" subgroup (consensus molecular subtype (CMS)-4), which accounts for 23% of all CRC, was initially believed to be due to features of the cancer cells themselves, such as a serrated cancer phenotype or a cancer stem cell phenotype. However, subsequent studies have shown that the genes associated with a poor prognosis are exclusively expressed by the microenvironment, more specifically the cancer-associated fibroblasts (CAFs) [2]. A major role for the microenvironment is also suggested by the finding that cancers displaying large quantities of tumor stroma have a worse prognosis [3–8].

Several lines of evidence point toward a central role for transforming growth factor-β (TGF-β) superfamily signaling in tumor/stroma interactions. First, the genes highly upregulated in mesenchymal-type CRC belong to the TGF-β superfamily. Second, microdissection of the tumor stroma combined with hypothesis-free analyses with proteomics or gene expression arrays consistently reveals high expression

These authors contributed equally: Sarah Ouahoud, Philip W. Voorneveld, Lukas J. A. C. Hawinkels, James C. H. Hardwick

Supplementary information The online version of this article (https://doi.org/10.1038/s41388-020-1157-z) contains supplementary material, which is available to authorized users.

✉ James C. H. Hardwick
J.C.H.Hardwick@LUMC.nl

[1] Department of Gastroenterology & Hepatology, Leiden University Medical Center, Leiden, The Netherlands

[2] Department of Surgery, Leiden University Medical Center, Leiden, The Netherlands

Published online: 23 January 2020

of TGF-β superfamily members, including the bone morphogenetic proteins (BMPs) [9, 10]. Third, our group has shown that the combination of large amounts of stroma, and the loss of mothers against decapentaplegic homolog 4 (SMAD4) expression in the tumor, is associated with an even poorer prognosis than either factor alone [11]. Previous research into the molecular mechanisms involved in the tumor/stroma interactions in CRC has focused heavily on the TGF-β pathway [12, 13]. This work has revealed an important role for a one-way tumor/stroma interaction where TGF-β secreted by fibroblasts promotes metastasis formation [12, 13]. In addition, whether this was dependent on the specific mutanome of the cancer cells, particularly the loss of SMAD4, was not investigated.

SMAD4 is the central signal transduction element of both the TGF-β and BMP-signaling pathway. The loss of SMAD4 occurs late in the adenoma-to-carcinoma sequence, and is seen in 30–40% of CRCs [14, 15]. Its loss is associated with the presence of liver metastases, a poor prognosis, and a poor response to chemotherapy [16–18]. While the consequences of SMAD4 loss could be due to the modulation of either the TGF-β or the BMP pathways, the BMP arm of the TGF-β superfamily has remained relatively under investigation in cancer, although interest is increasing [19]. In previous work, we have investigated the prometastatic effects of BMP signaling in SMAD4-negative cancers, and the pre-eminence of BMP signaling rather than TGF-β signaling in determining prognosis [20–23]. The potential role of BMPs in the tumor/stroma interactions, or to what extent the tumor/stroma interactions are two-way interactions, is poorly understood.

We therefore aimed to investigate how fibroblasts interact with CRC cells, focusing on the role of all TGF-β superfamily members including BMPs. We further studied the potential influence of loss of SMAD4 expression in the cancer cells on this interaction, by investigating both the influence of fibroblasts on the tumor cells, as well as the influence of the tumor cells on the fibroblasts. Our data show a BMP2-dependent reciprocal interaction between SMAD4-deficient tumor cells and fibroblasts, promoting CRC cell invasion, and metastasis formation. Furthermore, our data show that the cytokine tumor necrosis factor (TNF)-related apoptosis-inducing ligand (TRAIL), secreted by SMAD4-deficient tumor cells, might play a role in inducing fibroblast BMP2 expression.

Results

Fibroblasts stimulate the invasion of SMAD4-deficient colon cancer cells

To look for evidence of a SMAD4-dependent tumor-promoting tumor/stroma interaction, we first performed in vitro transwell invasion assays with either SMAD4-deficient HT29 cells or isogenic SMAD4-expressing HT29 cells, cocultured with fibroblasts. HT29 and the isogenic HT29 (HT29 S4) labeled with CellTracker were added to the upper well of a transwell system, while 18co fibroblasts or a medium without cells were placed in the bottom well. The fluorescent signal from the invaded cancer cells through the transwell filter was measured for 24 h. The presence of fibroblasts in the bottom well did not affect the invasion of the SMAD4-proficient HT29 cells compared with the medium alone. Importantly, SMAD4-expressing HT29 cells appear to have a lower basal and fibroblast-induced migratory capacity, when compared with SMAD4-deficient HT29 cells (Supplementary Fig. 1). In contrast, a significant threefold increase in invasion was observed in the SMAD4-deficient HT29 cells when fibroblasts were present in the bottom well compared with the medium alone (Fig. 1a, b). This increase in invasion was not due to an increase in proliferation, which was not significantly altered upon 18co fibroblast coculture (Supplementary Fig. 2). These data indicate that 18co fibroblasts can specifically stimulate SMAD4-deficient HT29 cell invasion.

Conditioned medium from SMAD4-deficient tumor cells increased fibroblast BMP2 expression

Previously, we have shown that BMP signaling loses its tumor-suppressing effect and drives metastasis in CRC cells without a functional SMAD4 protein [22]. This suggests an important role for TGF-β superfamily signaling, and we therefore reasoned that the factors involved would be expected to be TGF-β/BMP superfamily members. To investigate which fibroblast-derived factors could be responsible for the increase in CRC cell invasion, a TGF-β/BMP-specific qPCR array was used. Fibroblasts were exposed to conditioned medium (CM) from either SMAD4-deficient HT29 cells or SMAD4-proficient HT29 cells for 24 h, and a qPCR expression array was performed for 84 genes related to the TGF-β/BMP superfamily. The most differentially expressed, secreted ligand was found to be BMP2. BMP2 was upregulated 2.73-fold ($p = 0.037$) in fibroblasts stimulated with SMAD4-deficient HT29 CM, while it was found to be downregulated 14-fold by fibroblasts stimulated with SMAD4-proficient HT29 CM ($p = <0.001$) (Fig. 1c, d). This implies that SMAD4-deficient CRC cells can increase fibroblast BMP2 expression, and that BMP2 could be the secretory ligand secreted by fibroblasts that facilitate invasion.

Invasion of SMAD4-deficient cancer cells by fibroblasts is BMP2 dependent

Since BMP2 expression was specifically and strongly enhanced upon culture of 18co fibroblasts with SMAD4-

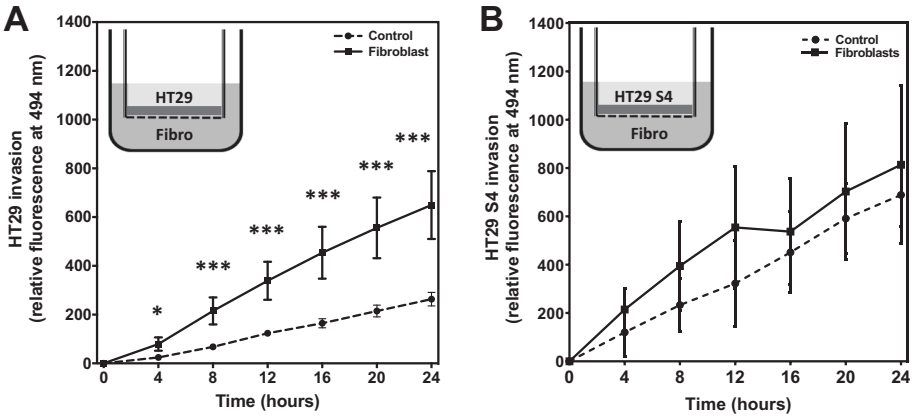

C HT29 SMAD4^{-} conditioned medium vs control medium

Top 10 upregulated genes in fibroblast

	Gene	Fold change	p-value
1	STAT1	4.33	2.82E-05
2	**BMP2**	**2.73**	**0.037**
3	IGF1	2.42	0.048
4	B2M	2.02	0.000
5	IL6	1.76	0.125
6	IGFBP3	1.62	0.039
7	BMP6	1.40	0.325
8	JUNB	1.40	0.227
9	BMP4	1.40	0.234
10	TGFB1	1.39	0.346

Top 10 downregulated genes in fibroblast

	Gene	Fold change	p-value
1	COL3A1	2.28	0.353
2	CHRD	2.23	0.320
3	LTBP4	2.05	0.046
4	DLX2	1.91	0.329
5	HIPK2	1.83	0.087
6	GAPDH	1.81	0.052
7	GDF6	1.76	0.099
8	HPRT1	1.72	0.501
9	ACVR2A	1.70	0.122
10	RPL13A	1.61	0.001

D HT29 SMAD4^{+} conditioned medium vs control medium

Top 10 upregulated genes in fibroblast

	Gene	Fold change	p-value
1	LTBP4	8.22	0.005
2	IL6	6.11	0.003
3	SMAD4	5.88	0.008
4	BAMBI	4.28	0.049
5	RPL13A	4.27	0.008
6	FST	4.08	0.008
7	ID1	3.69	0.016
8	FKBP1B	3.26	0.016
9	TGIF1	3.08	0.033
10	SMAD3	2.82	0.017

Top 10 downregulated genes in fibroblast

	Gene	Fold change	p-value
1	IGFBP3	33.33	0.017
2	COL3A1	20.00	0.019
3	COL1A1	20.00	0.004
4	BMPER	16.67	0.030
5	SOX4	14.29	0.048
6	**BMP2**	**14.29**	**0.000**
7	COL1A2	14.29	0.004
8	BMP4	11.11	0.029
9	JUNB	9.09	0.004
10	TGFB2	6.67	0.002

Fig. 1 SMAD4-deficient HT29 cells show increased invasiveness in the presence of fibroblasts. a The presence of fibroblasts in the bottom compartment of the transwell stimulated SMAD4-deficient HT29 cells to significantly invade more through the Matrigel-coated filter of the transwell compared with the control. **b** No differences in invasion were observed for SMAD4-proficient HT29 (HT29 S4) cell invasion upon the presence of fibroblasts. **c/d** The TGF-β/BMP-specific array, performed on RNA isolated from fibroblasts, showed that BMP2 (bold) was the highest upregulated secreted ligand in fibroblasts stimulated with SMAD4-deficient HT29 CM, while being downregulated 14-fold upon fibroblast stimulation with HT29 S4 CM. A representative experiment of three independent experiments in triplicate is shown (*$p \le 0.05$, **$p \le 0.01$, and ***$p \le 0.001$).

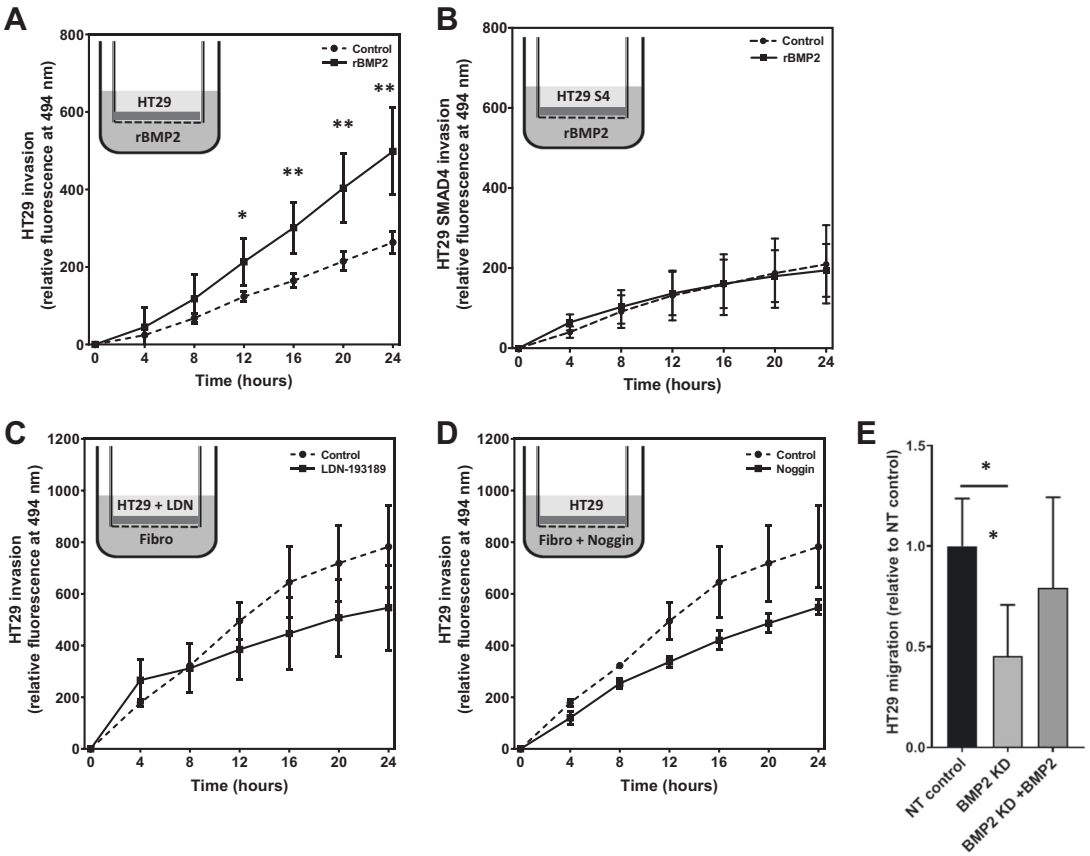

Fig. 2 Increased SMAD4-deficient HT29 invasion toward fibroblasts is BMP signaling dependent. a Replacing fibroblasts in the bottom compartment with recombinant human BMP2 (rBMP2) caused increased invasion of the SMAD4-deficient HT29 cells. **b** rBMP2 does not induce invasion of SMAD4-proficient HT29 cells. **c/d** Fibroblast-induced invasion was reverted upon addition of LDN-193189, a small molecule inhibitor for the type-I BMP receptor or the BMP antagonist Noggin. **e** BMP2-KD fibroblast does not increase SMAD4-deficient HT29 cell invasion, compared to the NT control, which can be rescued by the addition of recombinant human BMP2. The control condition shown in graphs **c** and **d** are identical as all conditions were included in the same experiment but divided into two graphs to increase clarity. A representative experiment of three independent experiments in triplicate is shown ($*p \leq 0.05$, $**p \leq 0.01$).

deficient HT29, we investigated whether fibroblast BMP2 secretion might explain the increase in SMAD4-deficient cancer cell invasion. SMAD4-proficient and SMAD4-deficient HT29 cells were seeded in the upper well of a Matrigel-coated transwell system, while 100 ng/ml recombinant human (r)BMP2 was added to the lower well. BMP2 stimulated the invasion of SMAD4-deficient HT29 cells, but did not affect invasion of SMAD4-proficient HT29 cells (Fig. 2a, b). Transwell invasion assays with the CRC cell lines DLD-1 and HCT116 (both SMAD4 positive) and their SMAD4-deficient equivalent confirmed specific increased invasion for the SMAD4-deficient cell lines to BMP2 (Supplementary Fig. 1).

To further investigate whether fibroblast-derived BMP2 is responsible for the increased invasion, cancer cells were seeded in the upper well and fibroblasts in the lower well with or without the addition of the BMP inhibitor Noggin, or the BMP receptor kinase inhibitor LDN-193189. The presence of either Noggin or LDN-193189 reverted the fibroblast-induced invasion of SMAD4-deficient HT29 cells (Fig. 2c, d). To specifically confirm the role of fibroblast-derived BMP2, we performed transwell assays using 18co fibroblasts with stable BMP2 shRNA mediated knockdown (KD) or a NT control in the bottom well. Significantly less migration of SMAD4-deficient CRC cells was observed with the BMP2-KD fibroblasts compared to the NT control (Fig. 2e). The migratory capacity was partially restored after the addition of rBMP2 to the BMP2-KD fibroblast (Fig. 2e and Supplementary Fig. 3). These results show that fibroblast-derived BMP2 might play an important role in increasing the invasive behavior of SMAD4-deficient cells.

Fibroblasts increase liver metastasis formation in a BMP2-dependent manner in vivo

The ability of fibroblasts to modulate the invasion and metastasis of CRC cells was further investigated by using a mouse model for experimental liver metastasis. Immunodeficient mice were co-injected intrasplenically with luciferase expressing SMAD4-deficient or SMAD4-proficient

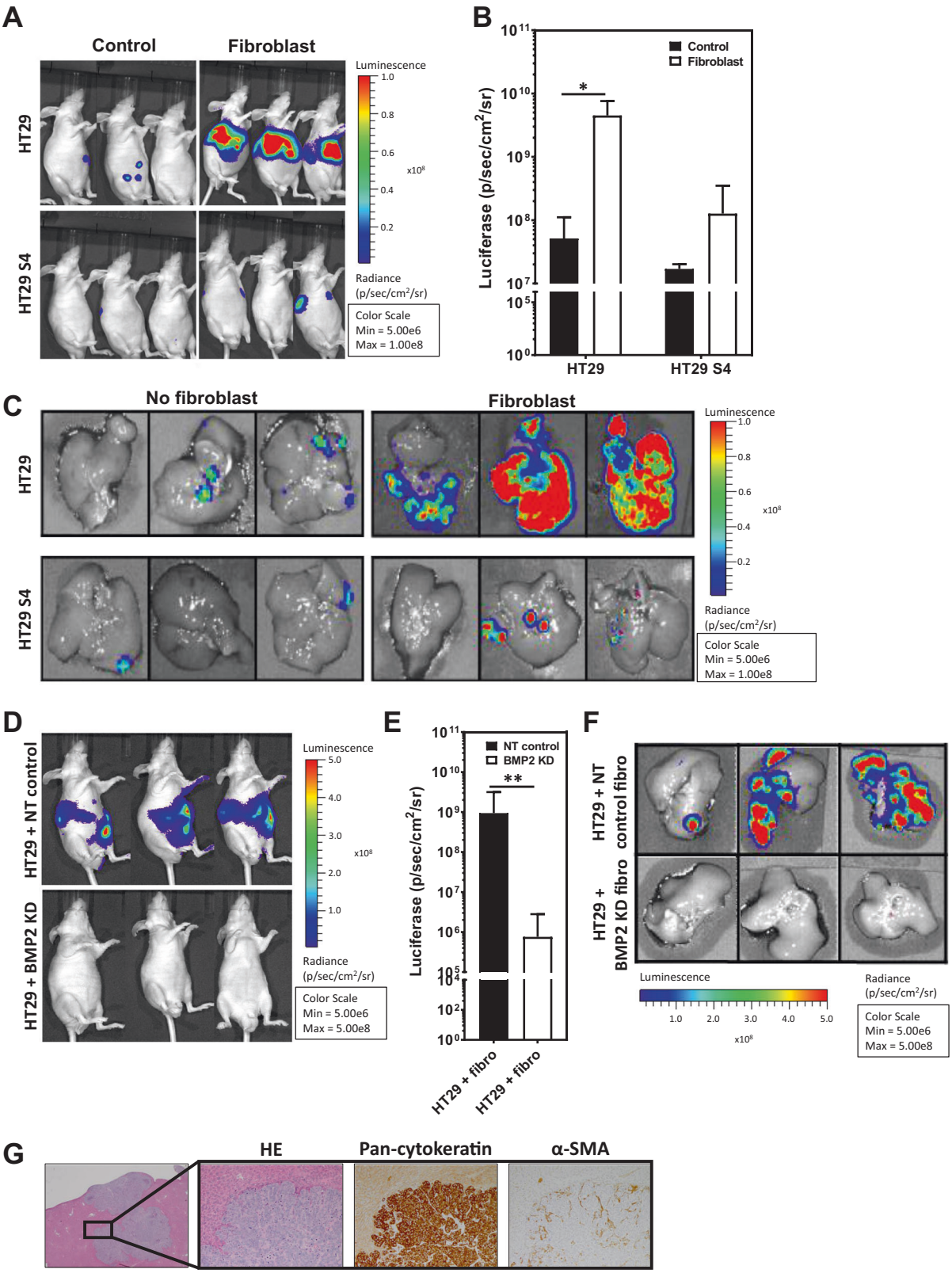

HT29 cells, with or without 18co fibroblasts. Liver metastasis formation was followed by bioluminescent imaging. Co-injection of fibroblasts led to a nonsignificant, fourfold increase in liver metastasis formation of SMAD4-proficient HT29 cells compared to mice injected with HT29 alone (Fig. 3a–c). In contrast, co-injection of fibroblasts together

◀ **Fig. 3 Fibroblast-derived BMP2 increased liver metastasis formation in mice. a/b** Co-injection of fibroblasts with SMAD4-deficient HT29 cells ($n = 5$) increased liver metastatic outgrowth. An 88-fold higher luciferase signal was observed in the co-injected mice when compared to the mice injected with HT29 cells only ($n = 4$; $p = 0.02$) while co-injection of SMAD4-proficient HT29 cells with fibroblast ($n = 4$) resulted in a not significant fourfold higher luciferase signal compared to mice injected with only SMAD4-proficient HT29 ($n = 4$; $p = 0.5$). **c** Confirmation of liver metastatic lesions ex vivo. **d/e/f** Co-injection of SMAD4-deficient HT29 cells with NT fibroblast results in liver metastatic outgrowth. Co-injecting mice with BMP2-KD fibroblast ($n = 10$) led to decreased metastatic burden compared to NT control ($n = 13$; $p = 0.008$). **g** Immunohistochemical staining of livers from mice co-injected with SMAD4-deficient HT29 cells and fibroblast for pan-cytokeratin and α-SMA verified the presence of epithelial cancer cells lesions, including α-SMA positive fibroblasts. Data are shown as the mean ± SD (*$p \le 0.05$, **$p \le 0.01$).

with SMAD4-deficient HT29 cells leads to an 88-fold higher luciferase signal ($p = 0.022$) compared with mice injected with SMAD4-deficient HT29 cells only. Ex vivo imaging of the livers confirmed that mice injected intrasplenically with both the fibroblast and SMAD4-deficient HT29 showed the highest liver metastatic load. Overall, these results show that liver metastasis formation is strongly enhanced when SMAD4-deficient CRC cells are co-injected with fibroblasts.

Since our in vitro studies suggest that BMP2 secreted by fibroblasts stimulates SMAD4-deficient CRC cell invasion, and BMP2 might be responsible for the prometastatic effects, we co-injected HT29 cells intrasplenically together with BMP2-KD- or non-targeting (NT) control fibroblast. Our data show that significantly less metastases were formed in mice which received HT29 cells together with BMP2-KD fibroblasts, compared to fibroblasts expressing a NT control ($p = 0.008$) (Fig. 3d–f). Histological analysis of the metastasis in the liver showed the presence of fibroblasts between the HT29 cells (Fig. 3g). However, due to cross-reactivity of the human α-SMA antibody with murine α-SMA, we cannot confirm that the fibroblasts are of either human or mouse origin. These data suggest that fibroblast-derived BMP2 stimulates liver metastasis formation of SMAD4-deficient CRC cells in vivo.

TRAIL is differentially expressed in SMAD4-deficient compared with SMAD4-proficient colorectal cancer cells

Having shown that fibroblasts influence SMAD4-deficient CRC cells by secreting BMP2, we continued investigating the second arm of this bidirectional interaction to determine how SMAD4-deficient cells influence fibroblasts. Since BMP2 expression was specifically enhanced by SMAD4-deficient CRC cell CM we reasoned that the secreted factors responsible might be differentially expressed by SMAD4-proficient vs SMAD4-deficient cell lines. To investigate this, an in silico analysis was performed on publicly available mRNA expression data of 26 human CRC cell lines, with established SMAD4 mutational status. Of the top 20 genes that were found to be differentially expressed in SMAD4-deficient CRC cell lines only two secreted factors, IL-13 and TRAIL, were identified (Fig. 4a).

To investigate if IL-13 or TRAIL could induce fibroblast BMP2 expression, we stimulated fibroblasts with recombinant human IL-13 or human TRAIL. Stimulation of fibroblasts with IL-13 did not induce BMP2 upregulation (Fig. 4b), while stimulation with TRAIL caused a strong and consistent upregulation of BMP2 in 18co fibroblasts (Fig. 4c) which could be blocked by adding a TRAIL neutralizing antibody. In addition, the extent of fibroblast BMP2 upregulation upon stimulation with CM from various CRC cells (Fig. 4d) seemed to correlate with their relative TRAIL expression (Fig. 4e, f). These data were confirmed in primary normal colonic fibroblast (NF) and CAFs. Stimulation with TRAIL or HT29 CM resulted in an induction of BMP2 expression in four out of six fibroblasts/CAF-pairs tested, although basal levels varied between different fibroblasts (supplementary Fig. 4). Stimulation of fibroblasts with TRAIL did not result in induction or downregulation of TGF-β1, TGF-β2, or TGF-β3 expression while it appeared to downregulate BMP4 (Fig. 4g, h). These results suggest that TRAIL increases fibroblast BMP2 expression, while decreasing BMP4 and leaving TGF-β ligand expression unaltered.

Stromal BMP2 expression is associated with poor patient survival in SMAD4-deficient CRC

The results from our in vitro and in vivo studies in mice suggest that BMP2 is prometastatic in SMAD4-deficient CRC cells. To investigate whether our experimental findings can be extrapolated to humans we analyzed the associations that these would predict in human CRC specimens.

The source of the BMP2 appears to be the CAFs where BMP2 secretion is stimulated by the presence of SMAD4-negative tumor cells. If this is true, we would predict that SMAD4 negative tumors with high stromal BMP2 would have a high propensity to metastasize resulting in a poor prognosis and reduced survival. We, therefore, investigated a panel of 146 stage III tumors from the Leiden University Medical Centre with relevant clinical data. We performed immunohistochemistry on tissue sections, including the invasive front of the tumor. Loss of SMAD4 expression in the tumor was associated with both poor overall survival (OS) (univariate: HR = 1.70 (0.52–2.80); $p = 0.03$ and multivariate: HR = 1.41 (1.02–2.82); $p = 0.04$) and disease-free survival (DFS) (univariate: HR = 1.75 (1.11–2.76); $p = 0.02$ and multivariate: HR = 1.62 (1.02–2.57);

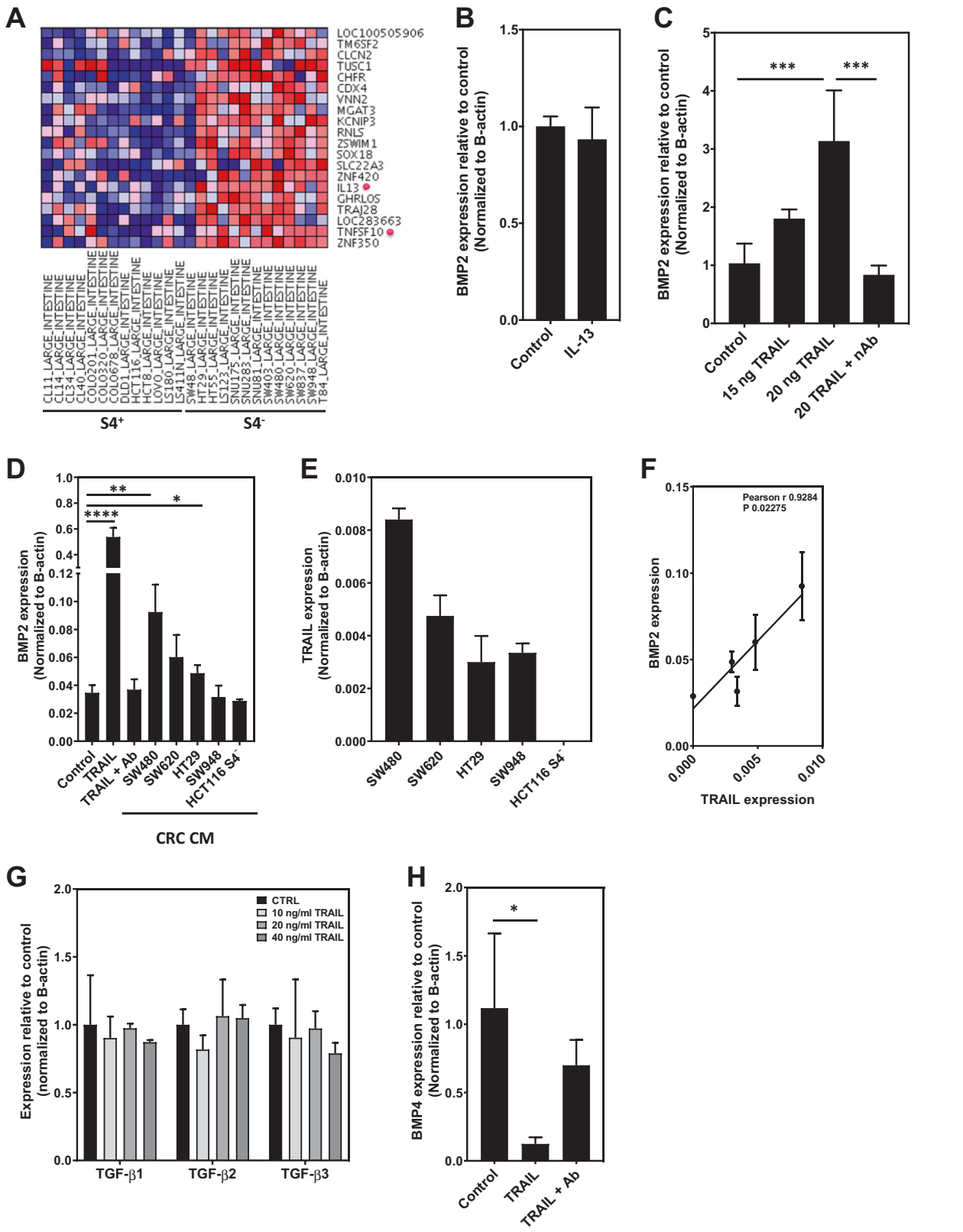

$p = 0.04$) (Table 1). BMP2 expression was observed in the stroma/fibroblasts at the invasive front of the tumor. High stromal BMP2 expression was found in 39.7% (58/146) of the stage III CRC samples, but by itself it was not significantly associated with OS (HR = 1.4 (0.91–2.21); $p = 0.06$) and DFS (HR = 1.15 (0.75–1.76); $p = 0.52$) (Table 1

◀ **Fig. 4 TRAIL, a cytokine upregulated in SMAD4-deficient CRC cell lines, regulates BMP2 expression in fibroblasts. a** An in silico analysis of genes differentially expressed between SMAD4-deficient/SMAD4-proficient CRC cell lines. Among these differentially expressed genes, only IL-13 and TRAIL (red dot) are secreted ligands. **b** Stimulation of fibroblast with 20 ng/ml IL-13 did not change BMP2 mRNA expression. **c** Stimulation of fibroblasts with TRAIL shows a dose-dependent induction of BMP2 ($p \le 0.001$). **d** Stimulation of fibroblasts with CRC CM resulted in an upregulation of BMP2, and **e/f** seem to correlate with TRAIL expression. **g/h** Stimulation of fibroblasts with TRAIL did not result in an upregulation or downregulation of TGF-β1, TGF-β2, and TGF-β3 but resulted in downregulation of BMP4. A representative experiment of three independent experiments in triplicate is shown ($*p \le 0.05$, $**p \le 0.01$, $***p \le 0.001$, and $****p \le 0.0001$).

and Supplementary Table 1) in the whole cohort. However, when we investigated the association between stromal BMP2 expression and tumor SMAD4 expression we found that high stromal BMP2 expression accompanied by loss of SMAD4 in the cancer epithelial cells was strongly associated with poor prognosis (OS: HR 1.81 (1.06–3.08); $p = 0.03$), adjusted HR 2.88 (1.05–8.13); $p = 0.04$ (Table 2 and Supplementary Table 2). Importantly, this association was specific for SMAD4-deficient cancer and not observed in SMAD4-proficient cancers with high stromal BMP2 expression (Fig. 5, OS: HR 0.86 (0.38–1.93); $p = 0.72$, adjusted HR 0.88 (0.39–1.99); $p = 0.76$). These data indicate that high stromal BMP2 expression is associated with poor patient survival in SMAD4-deficient CRC.

Discussion

In this study, we show evidence for a bidirectional crosstalk between fibroblasts and CRC cells that influences cancer cell invasion and metastasis formation. Our data suggest that SMAD4-deficient CRC cells overexpress TRAIL, which stimulates fibroblasts to secrete BMP2, which in turn stimulates SMAD4-deficient tumor cell migration, invasion, and metastasis formation. This may explain the previously described association between high amounts of tumor stroma, loss of SMAD4 expression, and poor prognosis [11].

The worst prognosis of patients with CRCs belonging to the "mesenchymal" CMS4 subgroup underlines the importance of the tumor stroma in stimulating cancer progression [1, 24], although they do not display the highest SMAD4 mutation rates. Sarshekeh et al. reported that the frequency of SMAD4 mutations was found in CMS3 (25%) followed by CMS1 (17.2%), CMS4 (6%), and lastly CMS2 (3.5%). However still the worse prognosis in the mesenchymal CMS4 subgroup provides the rationale for focusing efforts into further understanding of the molecular mechanisms underlying tumor progression in this aggressive subtype. To date most research in this area has concentrated on elucidating the role of TGF-β signaling. The potential role of the BMP-signaling pathway has remained largely unexplored, despite recent data showing that BMP-signaling gene sets are also upregulated specifically in mesenchymal CRC [25]. Previous research has also investigated CRC without subdividing into distinct molecular subtypes, while evidence would clearly suggest that the tumor/stroma interaction is highly dependent on the molecular tumor subtype. Next to that, gene expression analysis that does not take into account stromal or epithelial origin hampers the conclusions regarding the interaction between these cell types.

In this study, we have focused on SMAD4-deficient CRC. SMAD4-deficient CRCs exhibit the same hallmarks as mesenchymal CRC, being associated with increased metastasis formation and a poor prognosis. They also show high levels of Epithelial-to-Mesenchymal Transition (EMT), high TGF-β signaling, and large quantities of tumor stroma. There also seems to be a specific tumor/stroma interaction in this molecular subtype, as the presence of high amounts of stroma, or high stromal tumors, and loss of SMAD4 in the tumor, is associated with a worse prognosis than either feature alone [11].

This study builds on our previous work on the role of the BMP pathway in the intestine and in CRC. We have previously shown that BMP2 is usually expressed by epithelial cells in the normal intestinal epithelium where it counterbalances the effects of the Wnt pathway [20]. In previous studies, we have shown that loss of SMAD4 switches BMP signaling from being tumor suppressive to tumor enhancing by activation of EMT, and stimulating invasion and metastasis in CRC [22]. This and other studies in other tumor types indicate that despite being a tumor suppressive pathway in untransformed cells, BMP signaling exhibits a dual role in cancer similar to TGF-β and can act to promote tumor progression and metastasis formation in the later stages of tumorigenesis [22, 26, 27]. We now show that BMP2 can also be highly expressed in fibroblasts at the invasive front of late stage CRC. Interestingly, the SMAD4 negative tumors with low BMP2 expression have a similar prognosis to SMAD4 positive tumors. It is possible that the very poor prognosis of the BMP2 stroma-high/SMAD4-tumor-negative subgroup is actually responsible for the extensively described poor prognosis of SMAD4 negative tumors as a whole. The molecular mechanism is how fibroblast-derived BMP2 achieving its tumor-promoting effects could be activating non-SMAD signaling pathways, resulting in proliferation, migration, and invasion of SMAD4-deficient cancer cells [28–30]. In the adenoma to carcinoma sequence, the expression of SMAD4 is lost in the later stages leading to tumor promoting effects of TGF-β signaling. For the BMP pathway, similar mechanisms have been proposed by our group [22]. Interestingly, BMP2

Table 1 Univariate and multivariate-adjusted hazard ratios with 95% confidence intervals (CI) of potential CRC risk factors for overall survival and disease-free survival.

	Univariate		Multivariate	
	HR (95%)	*p* value	HR (95%)	*p* value
Overall survival				
Age (≥65 y vs. <65 y)	2.87 (1.77–4.64)	**<0.01**	2.02 (1.20–3.42)	**0.01**
Sex (male vs. female)	1.37 (0.87–2.15)	0.16	–	–
Adjuvant therapy (no vs. yes)	2.86 (1.60–5.13)	**<0.01**	2.44 (1.29–4.39)	**0.01**
Location (right vs. left)	1.45 (0.93–2.26)	0.10	1.41 (0.87–2.26)	0.16
Microsat. status (MSI vs. MSS)	1.07 (0.95–1.19)	0.85	–	–
Lymph nodes (N1 vs. N2)	1.60 (0.99–2.63)	0.07	1.50 (0.90–2.48)	0.12
SMAD4 tumor (neg vs. pos)	1.70 (0.52–2.80)	**0.03**	1.70 (1.02–2.82)	**0.04**
BMP2 stroma (high vs. low)	1.40 (0.91–2.21)	0.06	–	–
Disease-free survival				
Age (≥65 y vs. <65 y)	2.33 (1.49–3.63)	**<0.01**	1.81 (1.13–2.93)	**0.02**
Sex (male vs. female)	1.35 (0.88–2.08)	0.17	–	–
Adjuvant therapy (no vs. yes)	2.92 (1.52–5.59)	**<0.01**	1.95 (1.13–3.36)	**0.02**
Location (right vs. left)	1.22 (0.80–1.86)	0.35	–	–
Microsat. status (MSI vs. MSS)	1.08 (0.97–1.21)	0.82	–	–
Lymph nodes (N1 vs. N2)	1.59 (1.00–2.54)	0.052	1.56 (0.97–2.52)	0.07
SMAD4 tumor (neg vs. pos)	1.75 (1.11–2.76)	**0.02**	1.62 (1.02–2.57)	**0.04**
BMP2 stroma (high vs. low)	1.15 (0.75–1.76)	0.52	–	–

p-values that are statistically significant, are shown in bold.

exhibited a growth inhibitory effect on the COLO-357 cell line but lost its effect when a dominant-negative SMAD4 construct encoding for a truncated protein was introduced in these cells [28]. Non-SMAD TGF-β and BMP-dependent signaling leads to activation of, e.g., Rho family of small GTPases, MAPKs, PI3K, and TRAF 4/6. These pathways in general have been linked to cell proliferation, metastasis, and angiogenesis in several cancer types. Kleeff et al. also showed that BMP2 induced MAPK signaling in specifically SMAD4 mutant human pancreatic cell lines induces proliferation, while Jin et al. showed that BMP2 stimulation of the low SMAD4-expressing breast cancer cell line MCF-7 resulted in cytoskeletal reorganization, downregulation of surface E-cadherin and increased migratory and invasion capabilities [29]. How BMP2 can directly influence invasion is not yet fully understand, although for the SMAD4-deficient gastric cancer cell line AGS it has been shown that via activation of PI3K/AKT or MAPK pathway MMP9 expression was upregulated. In gastric tumor, biopsies for BMP2 and MMP9 showed a significant positive correlation with both lymph node metastasis and poorer prognosis, indicating a role for BMP2 induced MMP9 expression and subsequent tumor invasion [30].

In relation to intra- and extravasation, previous work identified BMP2 as a specific angiokine produced by liver sinusoidal endothelial cells (LSECs) [31]. During vascular dissemination these fibroblasts continue supporting the cancer cells until they have reached the liver. Extravasation in the liver is supported by the fibroblasts but might be rendered conducive due to the BMP2 expression by LSECs. During vascular dissemination these fibroblasts could continue supporting the epithelial cancer cells until they have reached the liver. Engraftment in the liver might be facilitated by fibroblasts but may also be enhanced by BMP2 expressed by LSECs [31]. This indicates that BMP2 might act at various levels to increase invasive and metastatic behavior.

In a screen for the molecular factors by which SMAD4-deficient cancers may influence fibroblasts, we identified TRAIL, a cytokine of the TNF ligand family. TRAIL has been described to be a potent inducer of apoptosis and since tumor cells seem to be significantly more sensitive to TRAIL-stimulated apoptosis than normal cells, the TRAIL pathway has been extensively studied as a possible therapeutic target for the treatment of cancer [32, 33]. We show that TRAIL induces fibroblast BMP2 expression that in turn enhances invasion and metastasis in SMAD4-deficient CRC cells. Anticancer therapy with TRAIL should therefore be considered cautiously, especially when it concerns tumors with a large stromal compartment and loss of SMAD4 where it could potentially have deleterious effects. How SMAD4 loss in linked to increased TRAIL expression is an intriguing question. TRAIL is already expressed by epithelial cells in normal colon [34]. For TGF-β, it has been shown that it induces TRAIL expression, but it fails to do so upon SMAD4 deletion or siRNA mediated downregulation

Table 2 Hazard ratios with 95% confidence intervals (CI) of tumor SMAD4 and stromal BMP2 expression on overall survival and disease-free survival.

	Stromal BMP2 expression		
	Low	High	*p* value
All cancers			
Overall survival			
Patients	88	58	
Deaths	49	38	
Hazard ratio (95%)	1.0 (reference)	1.42 (0.91–2.21)	0.12
Adjusted hazard ratio (95%)[a]	1.0 (reference)	1.26 (0.64–2.49)	0.51
Disease-free survival			
Patients	88	58	
Deaths	49	38	
Hazard ratio (95%)	1.0 (reference)	1.15 (0.75–1.76)	0.52
Adjusted hazard ratio (95%)[a]	1.0 (reference)	1.21 (0.60–2.42)	0.60
SMAD4-negative cancers			
Overall survival			
Patients	58	31	
Deaths	30	25	
Hazard ratio (95%)	1.0 (reference)	1.81 (1.06–3.08)	**0.03**
Adjusted hazard ratio (95%)[a]	1.0 (reference)	2.88 (1.05–8.13)	**0.04**
Disease-free survival			
Patients	58	31	
Deaths	35	25	
Hazard ratio (95%)	1.0 (reference)	1.58 (0.94–2.64)	0.08
Adjusted hazard ratio (95%)[a]	1.0 (reference)	1.50 (0.89–2.53)	0.13
SMAD4-positive cancers			
Overall survival			
Patients	30	27	
Deaths	11	13	
Hazard ratio (95%)	1.0 (reference)	0.86 (0.38–1.93)	0.72
Adjusted hazard ratio (95%)[a]	1.0 (reference)	0.88 (0.39–1.99)	0.76
Disease-free survival			
Patients	30	27	
Deaths	14	13	
Hazard ratio (95%)	1.0 (reference)	0.84 (0.39–1.79)	0.65
Adjusted hazard ratio (95%)[a]	1.0 (reference)	0.70 (0.33–1.54)	0.38

[a]Adjusted for sex, age, adjuvant therapy, lymph node status, location, and microsatellite status

Significant *p*-values are in bold.

[35, 36]. Multiple studies have reported the emergence of TRAIL resistance caused by alternative TRAIL signaling resulting in activation of NF-κB, upregulation of cFLIP, increase in the apoptotic proteins of the Bcl-2 family or the intracellular retention of TRAIL receptors [37–41]. SMAD4-deficient cells could have possibly upregulated their TRAIL expression to induce fibroblast BMP2 expression but also to create an autocrine survival loop as oncogenic TRAIL signaling has also been shown to promote survival. Further investigation is required to elucidate on a molecular level how SMAD4 loss is linked to increased TRAIL expression.

The long-term survival of patients with advanced CRC remains poor, despite recent advances in treatment. While multiple different therapeutic agents targeting the TGF-β pathway are under development for clinical use in CRC, there are currently no agents under development that target the BMP pathway [42]. This is in spite of the rapidly growing interest in BMP signaling in cancer. This study identifies new potential molecular targets specifically in poor prognosis mesenchymal CRC and would suggest that the development of cancer therapeutics targeting this area of cancer biology could be fruitful.

In conclusion, we propose the existence of a new pro-metastatic feedback loop in which SMAD4-deficient CRC cells produce TRAIL that stimulates fibroblasts to express BMP2. The fibroblast-derived BMP2 stimulates the invasion and metastasis of SMAD4-deficient CRC cells (Supplementary Fig. 5). These new findings could function as possible new therapeutic targets that could improve the long-term survival of patients with advanced CRC.

Methods

Cell culture, conditioned medium, and transfections

HT29, SW480, SW620, SW948, and HCT116 CRC cell lines and the colonic fibroblast cell lines CCD-18co were purchased from ATCC (American Type Culture collection, Manassas, VA). CRC cell lines were cultured in Dulbecco's modified Eagle's medium (DMEM) (Gibco, Paisley, Scotland), while 18co cells were cultured in DMEM/F12 GlutaMax (Gibco). Medium was supplemented with penicillin (50 U/ml, Gibco), streptomycin (50 µg/ml, Gibco), and 10% FCS (Gibco) unless stated otherwise. To generate CM subconfluent (75–85%), CRC cell lines were incubated with FCS-free DMEM for 5 days. After incubation, the medium was centrifuged for 5 min at 1200 rpm, and the supernatant was used for stimulation of fibroblasts. In addition, fibroblasts were seeded in six wells plates and stimulated for 24 h with recombinant human IL-13 (Peprotech Inc., London, UK) or recombinant human TRAIL (Peprotech) with

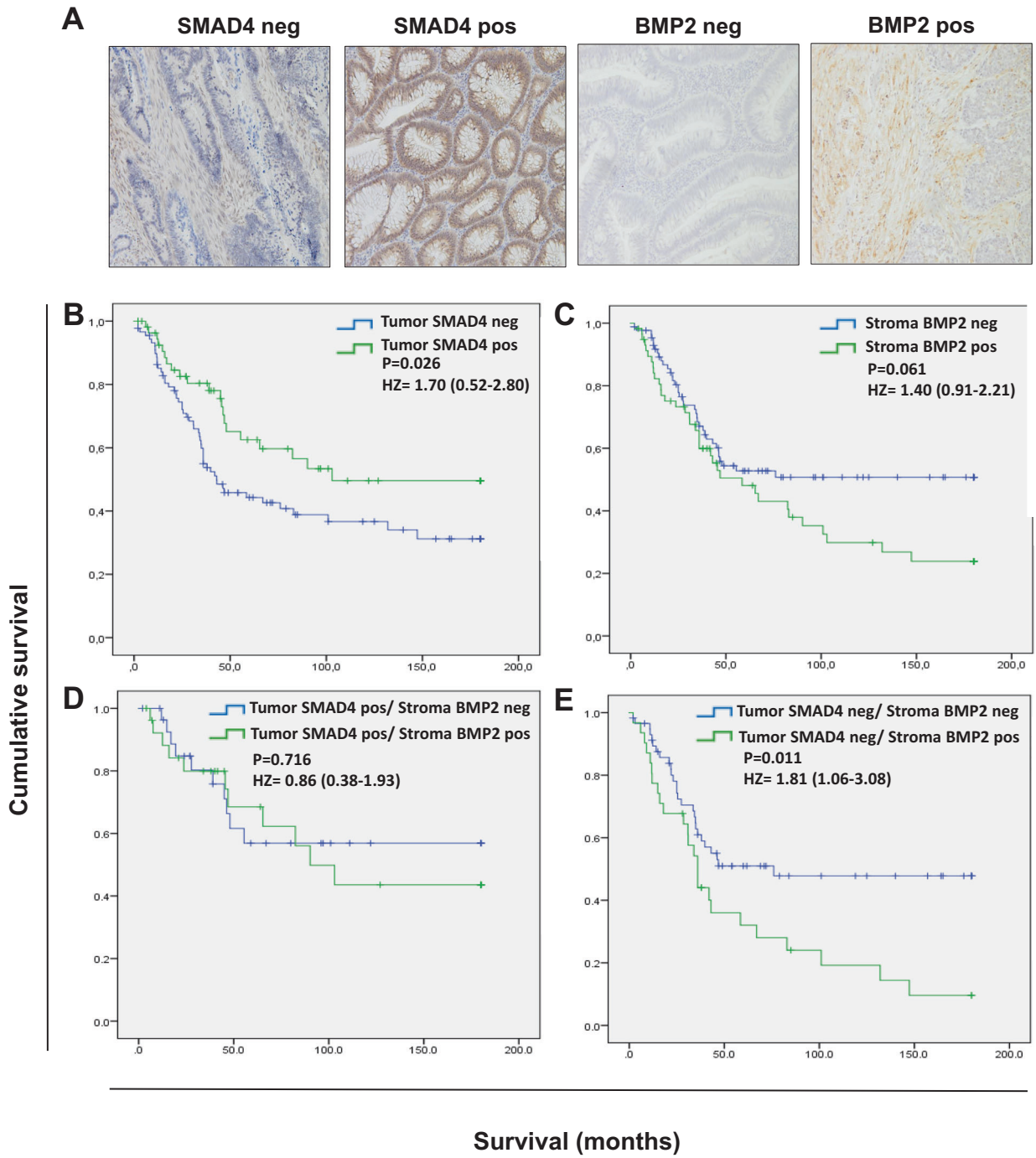

Fig. 5 The combination of stromal high BMP2 expression and epithelial SMAD4 loss predicts poor prognosis. a Representative examples of cases with SMAD4 negative (left panel) and positive (second panel), and low (third panel) and high (right panel) stromal BMP2 expression. **b** Patients with SMAD4-deficient tumors compared to patients with SMAD4-proficients tumors show decreased survival (univariate HR 1.70 (0.52–2.80); $p = 0.03$). **c** Stromal expression of BMP2 was associated with a non-significant poorer overall survival (HR 1.40 (0.91–2.21); $p = 0.06$). **d/e** The combination of high stromal BMP2 with SMAD4-deficient tumors predicts worse prognosis (HR 1.81 (1.06–3.08); $p = 0.01$). **e** This is not observed for high BMP2, SMAD4-proficient tumors (HR 0.86 (0.38–1.93); $p = 0.72$). HR are calculated with Cox regression analysis, while p values are calculated with the Kaplan–Meier.

or without 4 μg/ml antihuman TRAIL antibody (Peprotech) in serum free DMEM/F12.

Human CAFs were isolated from the nonnecrotic part of the tumors, whereas normal fibroblasts were isolated from adjacent healthy tissue. The tissue was washed with PBS, sectioned into 5-mm pieces, and enzymatically digested with a collagenase (Gibco) dispase II (Roche, Woerden, the Netherlands) mixture for 1 h at 37 °C. Cells were cultured in

complete DMEM/F12, and outgrowth of fibroblast-like cells was observed 2–5 days post isolation. Fibroblast identity and purity was confirmed by qPCR and protein analyses. Cells were used at passage 3–5.

Luciferase-expressing HT29 cells were generated by transducing HT29 with a pGL4 vector expressing firefly luciferase under control of the CAGGS promoter (Promega, Leiden, The Netherlands). Transfected cells were selected using 500 µg/ml neomycin. SMAD4-expressing HT29 cells were made by transfecting HT29 with a pcDNA3.1_SMAD4 vector [43]. BMP2-KD 18co fibroblasts were generated by transducing the cells lentivirally with vectors encoding BMP2 shRNA constructs (TRCN0000058193, Sigma mission shRNA library, Sigma-Aldrich, St. Louis, MO, USA) or a NT control. Transduced cells were selected by using 1.5 µg/ml puromycin (Sigma-Aldrich).

Invasion assays

Cells were labeled with CellTracker Green CMFDA (Invitrogen, Breda, The Netherlands), and transferred to 8-µm pore-size HTS FluorBlok cell culture inserts (BD Falcon, Breda, The Netherlands) pre-coated with 100 µl of 1:1 mix of Matrigel (BD Biosciences, Breda, The Netherlands) and serum-free DMEM in 24-well plates (Corning, NY, USA) containing DMEM. The fluorescent signal of the cells that had invaded trough the transwells was measured every 4 h for 24 h with the BioTek Flx800 (BioTek, Winooski, VT, USA). Data were corrected for background fluorescence and migration start points were set to zero.

MTS proliferation assay

HT29 cells (1500 cells per well) were seeded in triplicate in 96-well plates. After 24 h, medium was replaced with 100 µl 0.5% FCS/DMEM, 10% FCS/DMEM or 18co CM in 0.5% FCS/DMEM. At indicated time points, 20 µl of MTS substrate (Promega, Madison, WI, USA) was added to each well, and absorbance was measured at 490 nm (PerkinElmer, Groningen, The Netherlands) with the Cytation 5 image reader (Biotek, Winooski, VT, USA).

TGF-β/BMP-specific qPCR array

Fibroblasts were seeded in six-well plates and stimulated overnight with 2-ml CRC cell-derived, serum-free CM. The next day the cells were harvested and RNA was isolated using Trizol (Invitrogen) according to the manufacturer's instructions. Then a TGF-β/BMP-Signaling Pathway PCR array (PAHS-035D, SABiosciences, MD, USA) was performed according to the manufacturer's instructions.

Experimental liver metastasis mouse model

All animal experiments performed were approved by the animal welfare committee of the Leiden University Medical Center (LUMC) and conducted according to the recommendations and guidelines set by the LUMC and by the Dutch Experiments on Animals Act that serves the implementation of "Guidelines on the protection of experimental animals" by the European council. Experiments were performed as described before [44]. Animal sample sizes for the experiments were calculated using an alpha of 0.05 and a power of 80%, and mice were not randomized (and investigators were therefore not blinded) into treatment groups. In short, 6-week-old male immunocompromised Crl:CD1-Fox1nu mice (Charles River laboratories International, MA, USA) were injected intrasplenically with 1×10^6 luciferase expressing HT29 cells together ($n = 5$) or without 1×10^5 fibroblasts (nontransduced ($n = 5$), NT shRNA ($n = 13$) or BMP2 shRNA ($n = 10$)) in 100 µl 1× PBS. To follow metastases formation and growth, mice received an intraperitoneal injection with 100 mg/kg D-Luciferin twice weekly and imaged using the IVIS (PerkinElmer, MA, USA). Analyses were performed using the Living Image 3.2 software.

Immunohistochemical staining and analysis

Paraffin-embedded tissue samples were obtained from the Department of Pathology, LUMC, used according to the guidelines of the Medical Ethical Committee of the LUMC, and conducted in accordance to the Declaration of Helsinki and the Code of Conduct for responsible use of Human Tissue and Medical Research, as drawn up by the Federation of Dutch Medical Societies in 2011. This code permits the further use of coded residual (historical) tissue and data from the diagnostic process for scientific purposes. Permission is granted by implementing an opt-out procedure for the patients, written informed consent is in that case not needed.

Formalin-fixed paraffin-embedded primary tumor tissues from 146 stage III CRC patients between the years 1995 and 2011 were collected for which follow-up data were available. Embedded tumors were sectioned and stained immunohistochemically for BMP2 and SMAD4 as described before [45]. In short, slides were deparaffinized and rehydrated, after which antigen retrieval was performed by boiling slides in Tris EDTA (pH = 9.0) for 30 min for SMAD4 and sodium citrate (pH = 6.0) for 10 min. Slides were then blocked and incubated with mouse-anti-SMAD4 or goat-anti-BMP2 antibodies (Santa Cruz Biotechnology, Santa Cruz, CA, USA) for 60 min. Slides were washed and incubated for 60 min with the appropriate secondary antibody. Peroxidase activity was detected by FastDAB

(Sigma-Aldrich, Zwijndrecht, The Netherlands), and slides were counterstained with Hematoxylin (Sigma-Aldrich). Analysis of the stained slides was performed independently by two investigators in a blinded fashion. Expression of SMAD4 was scored as 0, no staining; 1, weak nuclear staining or no nuclear staining accompanied with weak membranous or cytoplasmic staining in <10% of the cells; 2 moderate to strong membranous or cytoplasmic staining in >10% of the cells. BMP2 was scored as negative when less than 30% of the cells showed positive staining.

In silico analysis

Data from the Cancer Cell Line Encyclopedia provided by the Broad Institute were loaded in the differential expression tool (https://portals.broadinstitute.org/ccle/home) to compare global gene expression in SMAD4-positive cell lines with SMAD4-negative cell lines.

Real-time quantitative PCR analysis

Total RNA was isolated using NucleoSpin RNA isolation kit (Macherey-Nagel, Germany), according to the manufacturer's instructions. cDNA was synthesized with the RevertAid First strand cDNA synthesis kit (Thermo Fisher Scientific). Real-time quantitative PCR was performed with SYBR Green Master mix (Bio-Rad laboratories, Nazareth, Belgium) using the iCycler Thermal Cycler and iQ5 Multicolour Real-Time PCR Detection System (Bio-Rad). Primers used for BMP2 were (fw 5′-GCAGGCACTCAGG TCAG-3′ and rev 5′-ATTCGGTGATGGAAACTGC-3′) and TRAIL (fw 5′-CCTGCGTGCTGATCGTGAT-3′ and rev 5′-ACGGAGTTGCCACTTGACTTG-3′). CT values were normalized to β-actin (fw 5′-GCAGGCACTCAGG TCAG-3′ and rev 5′-ATTCGGTGATGGAAACTGC-3′) or GAPDH (fw 5′-GCAGGCACTCAGGTCAG-3′ and rev 5′-ATTCGGTGATGGAAACTGC-3′).

Statistical analyses

Statistical analyses were performed by using either SPSS (version 20.0 for Windows, IBM SPSS statistics) or GraphPad Prism (version 7, GraphPad Software). Cox regression analysis was performed for OS and DFS. For the univariate and multivariate analysis, p values are based on Chi-square tests and are two-sided. A students t-test or one-way ANOVA was used for the calculation of other p values. Nonparametric variants of the students t-test or one-way ANOVA were used when data were abnormally distributed. A p value < 0.05 was considered statistically significant. Adjustments for potential confounders sex, age, adjuvant therapy, microsatellite stability status, lymph node status, (N1/N2) and tumor location (right/left) were made for the multivariate analysis.

Compliance with ethical standards

Conflict of interest The authors declare that they have no conflict of interest.

Publisher's note Springer Nature remains neutral with regard to jurisdictional claims in published maps and institutional affiliations.

References

1. Guinney J, Dienstmann R, Wang X, de Reyniès A, Schlicker A, Soneson C, et al. The consensus molecular subtypes of colorectal cancer. Nat Med. 2015;21:1350.
2. Calon A, Lonardo E, Berenguer-Llergo A, Espinet E, Hernando-Momblona X, Iglesias M, et al. Stromal gene expression defines poor-prognosis subtypes in colorectal cancer. Nat Genet. 2015;47:320.
3. Mesker WE, Junggeburt JM, Szuhai K, de Heer P, Morreau H, Tanke HJ, et al. The carcinoma-stromal ratio of colon carcinoma is an independent factor for survival compared to lymph node status and tumor stage. Cell Oncol. 2007;29:387–98.
4. Dekker TJA, van de Velde CJH, van Pelt GW, Kroep JR, Julien JP, Smit VTHBM, et al. Prognostic significance of the tumor-stroma ratio: validation study in node-negative premenopausal breast cancer patients from the EORTC perioperative chemotherapy (POP) trial (10854). Breast Cancer Res Treat. 2013;139:371–9.
5. Huijbers A, Tollenaar RAEM, v Pelt GW, Zeestraten ECM, Dutton S, McConkey CC, et al. The proportion of tumor-stroma as a strong prognosticator for stage II and III colon cancer patients: validation in the VICTOR trial. Ann Oncol. 2013;24:179–85.
6. Wang K, Ma W, Wang J, Yu L, Zhang X, Wang Z, et al. Tumor-stroma ratio is an independent predictor for survival in esophageal squamous cell carcinoma. J Thorac Oncol. 2012;7:1457–61.
7. Lv Z, Cai X, Weng X, Xiao H, Du C, Cheng J, et al. Tumor–stroma ratio is a prognostic factor for survival in hepatocellular carcinoma patients after liver resection or transplantation. Surgery. 2015;158:142–50.
8. Liu J, Liu J, Li J, Chen Y, Guan X, Wu X, et al. Tumor–stroma ratio is an independent predictor for survival in early cervical carcinoma. Gynecol Oncol. 2014;132:81–6.
9. Chen SX, Xu XE, Wang XQ, Cui SJ, Xu LL, Jiang YH, et al. Identification of colonic fibroblast secretomes reveals secretory factors regulating colon cancer cell proliferation. J Proteom. 2014;110:155–71.
10. Karagiannis GS, Berk A, Dimitromanolakis A, Diamandis EP. Enrichment map profiling of the cancer invasion front suggests regulation of colorectal cancer progression by the bone morphogenetic protein antagonist, gremlin-1. Mol Oncol. 2013;7:826–39.
11. Mesker WE, Liefers G-J, Junggeburt JMC, van Pelt GW, Alberici P, Kuppen PJK, et al. Presence of a high amount of stroma and downregulation of SMAD4 predict for worse survival for stage I-II colon cancer patients. Cell Oncol. 2009;31:169–78.
12. Calon A, Espinet E, Palomo-Ponce S, Tauriello DV, Iglesias M, Cespedes MV, et al. Dependency of colorectal cancer on a TGF-beta-driven program in stromal cells for metastasis initiation. Cancer Cell. 2012;22:571–84.
13. Tauriello DVF, Palomo-Ponce S, Stork D, Berenguer-Llergo A, Badia-Ramentol J, Iglesias M, et al. TGFbeta drives immune evasion in genetically reconstituted colon cancer metastasis. Nature. 2018;554:538–43.
14. Alazzouzi H, Alhopuro P, Salovaara R, Sammalkorpi H, Jarvinen H, Mecklin JP et al. SMAD4 as a prognostic marker in colorectal

cancer. Clin Cancer Res. 2005;11:2606–11. https://doi.org/10.1158/1078-0432.CCR-04-1458.
15. Kodach LL, Bleuming SA, Musler AR, Peppelenbosch MP, Hommes DW, van den Brink GR, et al. The bone morphogenetic protein pathway is active in human colon adenomas and inactivated in colorectal cancer. Cancer. 2008;112:300–6.
16. Alhopuro P, Alazzouzi H, Sammalkorpi H, Davalos V, Salovaara R, Hemminki A, et al. SMAD4 levels and response to 5-fluorouracil in colorectal cancer. Clin Cancer Res. 2005;11:6311–6.
17. Miyaki M, Iijima T, Konishi M, Sakai K, Ishii A, Yasuno M, et al. Higher frequency of Smad4 gene mutation in human colorectal cancer with distant metastasis. Oncogene. 1999;18:3098–103.
18. Papageorgis P, Cheng K, Ozturk S, Gong Y, Lambert AW, Abdolmaleky HM, et al. Smad4 inactivation promotes malignancy and drug resistance of colon cancer. Cancer Res. 2011;71:998–1008.
19. Wakefield LM, Hill CS. Beyond TGFbeta: roles of other TGFbeta superfamily members in cancer. Nat Rev Cancer. 2013;13:328–41.
20. Hardwick JC, Van Den Brink GR, Bleuming SA, Ballester I, Van Den Brande JM, Keller JJ, et al. Bone morphogenetic protein 2 is expressed by, and acts upon, mature epithelial cells in the colon. Gastroenterology. 2004;126:111–21.
21. Kodach LL, Wiercinska E, de Miranda NF, Bleuming SA, Musler AR, Peppelenbosch MP, et al. The bone morphogenetic protein pathway is inactivated in the majority of sporadic colorectal cancers. Gastroenterology. 2008;134:1332–41.
22. Voorneveld PW, Kodach LL, Jacobs RJ, Liv N, Zonnevylle AC, Hoogenboom JP, et al. Loss of SMAD4 alters BMP signaling to promote colorectal cancer cell metastasis via activation of Rho and ROCK. Gastroenterology. 2014;147:196–208 e113.
23. Hardwick JC, Kodach LL, Offerhaus GJ, van den Brink GR. Bone morphogenetic protein signalling in colorectal cancer. Nat Rev Cancer. 2008;8:806–12.
24. Dienstmann R, Vermeulen L, Guinney J, Kopetz S, Tejpar S, Tabernero J. Consensus molecular subtypes and the evolution of precision medicine in colorectal cancer. Nat Rev Cancer. 2017;17:79.
25. Irshad S, Bansal M, Guarnieri P, Davis H, Al Haj Zen A, Baran B, et al. Bone morphogenetic protein and Notch signalling crosstalk in poor-prognosis, mesenchymal-subtype colorectal cancer. J Pathol. 2017;242:178–92.
26. Katsuno Y, Hanyu A, Kanda H, Ishikawa Y, Akiyama F, Iwase T, et al. Bone morphogenetic protein signaling enhances invasion and bone metastasis of breast cancer cells through Smad pathway. Oncogene. 2008;27:6322.
27. Jiramongkolchai P, Owens P, Hong CC. Emerging roles of the bone morphogenetic protein pathway in cancer: potential therapeutic target for kinase inhibition. Biochem Soc Trans. 2016;44:1117–34.
28. Kleeff J, Maruyama H, Ishiwata T, Sawhney H, Friess H, Büchler MW, et al. Bone morphogenetic protein 2 exerts diverse effects on cell growth in vitro and is expressed in human pancreatic cancer in vivo. Gastroenterology. 1999;116:1202–16.
29. Jin H, Pi J, Huang X, Huang F, Shao W, Li S, et al. BMP2 promotes migration and invasion of breast cancer cells via cytoskeletal reorganization and adhesion decrease: an AFM investigation. Appl Microbiol Biotechnol. 2012;93:1715–23.
30. Kang MH, Oh SC, Lee HJ, Kang HN, Kim JL, Kim JS, et al. Metastatic function of BMP-2 in gastric cancer cells: the role of PI3K/AKT, MAPK, the NF-κB pathway, and MMP-9 expression. Exp Cell Res. 2011;317:1746–62.
31. Koch P-S, Olsavszky V, Ulbrich F, Sticht C, Demory A, Leibing T, et al. Angiocrine Bmp2 signaling in murine liver controls normal iron homeostasis. Blood. 2017;129:415.
32. Lemke J, von Karstedt S, Zinngrebe J, Walczak H. Getting TRAIL back on track for cancer therapy. Cell Death Differ. 2014;21:1350.
33. Johnstone RW, Frew AJ, Smyth MJ. The TRAIL apoptotic pathway in cancer onset, progression and therapy. Nat Rev Cancer. 2008;8:782.
34. Koornstra JJ, Kleibeuker JH, van Geelen CMM, Rijcken FEM, Hollema H, de Vries EGE, et al. Expression of TRAIL (TNF-related apoptosis-inducing ligand) and its receptors in normal colonic mucosa, adenomas, and carcinomas. J Pathol. 2003;200:327–35.
35. Herzer K, Grosse-Wilde A, Krammer PH, Galle PR, Kanzler S. Transforming growth factor-β-mediated tumor necrosis factor-related apoptosis-inducing ligand expression and apoptosis in hepatoma cells requires functional cooperation between smad proteins and activator Protein-1. Mol Cancer Res. 2008;6:1169–77.
36. Cortez VS, Ulland TK, Cervantes-Barragan L, Bando JK, Robinette ML, Wang Q., et al. SMAD4 impedes the conversion of NK cells into ILC1-like cells by curtailing non-canonical TGF-β signaling. Nature Immunology. 2017;18:995–1003.
37. Zhang L, Fang B. Mechanisms of resistance to TRAIL-induced apoptosis in cancer. Cancer Gene Therapy. 2005;12:228–37.
38. Lane D, Cartier A, L'Espérance S, Côté, M, Rancourt C, Piché A. Differential induction of apoptosis by tumor necrosis factor-related apoptosis-inducing ligand in human ovarian carcinoma cells. Gynecologic Oncology. 2004;93:594–604.
39. Lee T-J, Lee JT, Park J-W, Kwon TK. Acquired TRAIL resistance in human breast cancer cells are caused by the sustained cFLIPL and XIAP proteinlevels and ERK activation. Biochemical and Biophysical Research Communications. 2006;351:1024–30.
40. Wenger T, Mattern J, Penzel R, Gassler N, Haas TL, Sprick MR., et al. Specific resistance upon lentiviral TRAIL transfer by intracellular retention of TRAIL receptors. Cell Death & Differentiation. 2006;13:1740–51.
41. Song JH, Tse MCL, Bellail A, Phuphanich S, Khuri F, Kneteman NM., et al. Lipid rafts and nonrafts mediate tumor necrosis factor-related apoptosis-inducing ligand-induced apoptotic and non-apoptotic signals in non-small cell lung carcinoma cells. Cancer Research. 2007;67:6946.
42. Hawinkels LJAC, ten Dijke P. Exploring anti-TGF-β therapies in cancer and fibrosis. Growth Factors. 2011;29:140–52.
43. Voorneveld PW, Stache V, Jacobs RJ, Smolders E, Sitters AI, Liesker A, et al. Reduced expression of bone morphogenetic protein receptor IA in pancreatic cancer is associated with a poor prognosis. Br J Cancer. 2013;109:1805–12.
44. Paauwe M, Schoonderwoerd MJA, Helderman RFCPA, Harryvan TJ, Groenewoud A, van Pelt GW et al. Endoglin expression on cancer-associated fibroblasts regulates invasion and stimulates colorectal cancer metastasis. Clin Cancer Res. 2018. https://doi.org/10.1158/1078-0432.CCR-18-0329.
45. Voorneveld PW, Kodach LL, Jacobs RJ, van Noesel CJM, Peppelenbosch MP, Korkmaz KS, et al. The BMP pathway either enhances or inhibits the Wnt pathway depending on the SMAD4 and p53 status in CRC. Br J Cancer. 2014;112:122.